Epileptic seizures: Quakes of the brain?

Ivan Osorio,[1,2,*] Mark G. Frei,[2,†] Didier Sornette,[3,‡] John Milton,[4,§] and Ying-Cheng Lai[5,‖]
[1]*Department of Neurology, The University of Kansas Medical Center, 3599 Rainbow Boulevard, Mailstop 2012, Kansas City, Kansas 66160, USA*
[2]*Flint Hills Scientific, 5040 Bob Billings Parkway, Suite A, Lawrence, Kansas 66049, USA*
[3]*D-MTEC, D-PHYS and D-ERDW, ETH Zurich, Kreuzplatz 5, CH-8032 Zurich, Switzerland*
[4]*W.M. Keck Science Center, The Claremont Colleges, 925 North Mills Avenue, Claremont, California 91711, USA*
[5]*School of Electrical Computer and Energy Engineering, Department of Physics, Arizona State University, Tempe, Arizona 85287-5706, USA*

(Received 20 September 2009; revised manuscript received 12 July 2010; published 20 August 2010)

A dynamical analogy supported by five scale-free statistics (the Gutenberg-Richter distribution of event sizes, the distribution of interevent intervals, the Omori and inverse Omori laws, and the conditional waiting time until the next event) is shown to exist between two classes of seizures ("focal" in humans and generalized in animals) and earthquakes. Increments in excitatory interneuronal coupling in animals expose the system's dependence on this parameter and its dynamical transmutability: moderate increases lead to power-law behavior of seizure energy and interevent times, while marked ones to scale-free (power-law) *coextensive* with characteristic scales and events. The coextensivity of power law and characteristic size regimes is predicted by models of coupled heterogeneous threshold oscillators of relaxation and underscores the role of coupling strength in shaping the dynamics of these systems.

DOI: 10.1103/PhysRevE.82.021919 PACS number(s): 87.19.xm, 89.75.Da

I. INTRODUCTION

Power-law behaviors arise in a wide range of natural and artificial phenomena ranging from living neural populations [1] to earthquakes and forest fires [2–9]. It has been contended that the fact that all of these systems generate power laws stems from their common underlying structure, i.e., all are composed of interacting ("coupled") nonlinear relaxational threshold oscillators.[1] It is further contended that (1) although "closely related on a formal level," the systems generating these phenomena have "distinct collective properties" ranging from systemwide synchronization to self-organized criticality (SOC) [9] and (2) their constituent elements are strongly correlated and their near-mean field-driven threshold behavior arises from the underlying locally ergodic dynamics [10].

Using neuronal cultures and cortical rat slices, Beggs and Plenz [1] found that the size of local field potentials generated by these preparations have, as earthquakes and avalanches, no characteristic scale, and their probability density function (pdf) is described by a power law with an exponent of $-3/2$. This finding led to the postulate that "neuronal avalanches" (under nonexcited conditions) may be a generic property of cortical networks. However, this power law was destroyed by application to the culture of strychnine, a compound that enhances neuronal excitability, underscoring the sensitive dependence of scale-free behavior on conditions, specifically on the level of excitatory neuronal coupling, while suggesting the existence of metastable states in the said preparation. Other studies claim the existence of power-law behaviors in the brains of subjects with epilepsy. To wit, Worrell *et al.* [11] analyzed the voltages recorded (1 h segments) from the brains of seven humans with epilepsy. The resulting probability distribution of neuronal energy was argued to be a power law. However, the log-log plots linearity encompassed just over *1 decade*. Of note, these segments did *not* contain *seizures*. This same group [12] performed detrended fluctuation analysis of energy variability in 20 min recordings (*before* and *after* seizures) of human epileptogenic hippocampus activity, allegedly uncovering long-range temporal correlations with power-law scaling. These investigators concluded that their finding resembled that characterizing alpha rhythms recorded from the scalp of normal nonepileptic subjects during relaxed wakefulness and eyes closed [13]. This claim of similarity [12] is vexing given the notable differences in structure, function, state (pathological versus normal), and mode of recording (intracranial versus scalp) between normal thalamocortical alpha and abnormal hippocampal rhythms. Also, their statement ("long-range

*iosorio@kumc.edu
†frei@fhs.lawrence.ks.us
‡dsornette@ethz.ch
§jmilton@jsd.claremont.edu
‖ying-cheng.lai@asu.edu

[1]The term "relaxational threshold" is applied to phenomena with a disproportionately long (hours to years) charging or loading process vis-à-vis the very short (seconds to minutes) discharge of the accumulated energy. For instance, in the case of earthquakes, the slow motion of tectonic plates at typical velocities of a few cm/year accumulates strains in the core of locked faults over hundreds to thousands of years, which are suddenly relaxed by the meter-size slips occurring in seconds to minutes that define large earthquakes. Thus, one fault taken in isolation is genuinely a single relaxation threshold oscillator, alternating long phases of loading, and short slip relaxations (the earthquakes). While less well studied than earthquakes, the long (hours to years) interval between seizures and their short duration (rarely over 2 min) interpreted in light of the fact that the brain is composed of relaxational threshold oscillators (neurons) supports the notion that seizures too are also relaxational phenomena.

temporal correlation with power-law scaling is a fundamental feature of human brain activity") is troublesome as it would suggest that either scaling exponents do not provide meaningful information about different specific regimes of systems' dynamics (the brain in this case) or the manifest differences in certain emergent properties between certain neuronal networks are merely epiphenomenological. *Except* numerical simulations [9], *in vitro* experimentation [1] and the recent observation that the pdf of seizure energy in humans obeys a power law [14] but with an exponent (−5/3), distinct from that reported for dissociated neurons (−3/2) [1], suggest otherwise.

While claims of self-similarity and self-organized criticality unify this small body of literature, limitations either conceptual [11,12] or inherent to the experimental paradigm [1,9,10] or design [11,12] fragment it. The small size of the cohort, the short segment durations (40–60 min), and the lumping (into the analysis) of multifarious states and "events" [11,12] likely yield a narrow and hazy dynamical portrait.

The purported resemblances between earthquakes and neuronal spiking have neither been subjected to rigorous scrutiny nor have the properties been specified upon which the claims of similarity are made. Furthermore, even if the proof in support of the claim of dynamical similarities would have been furnished, the salient issue of extensibility to more complex intact systems such as the mammalian brain and the earth's crust remains unaddressed. The marked sensitivity of these systems' emergent properties to even minute changes in parameters and boundary conditions [9,10] and the limitations inherent to the modeling process of neural systems where network properties play a paramount role in the behavior of certain observables provide strong impetus for a systematic inquiry into the plausibility of these presumptive analogies. Despite the limitations mentioned above and others that will be expounded on below, these studies [1,9–12] raise the possibility that the behavior of neuronal assemblies and of epileptogenic regions is fractal in nature and that the observable (changes in neuronal voltages in dissociated or naturally assembled, but disturbed neurons) has no typical scale, that is, it is self-similar. In this context, the present study endeavors to (a) probe systematically and quantitatively the validity and relevance of claims of dynamical analogies between a type of neural activity (seizures) and earthquakes and, if present, identify which properties are shared by these two observables; (b) investigate in animals the role of coupling strength in shaping the behavior of neuronal oscillators and of the probability distribution function of seizures; and (c) test the robustness of a dynamical prediction derived from the dynamical analogy between seizures and earthquakes.

II. METHODS

A. Rationale for choice of experimental paradigm

Seizures which in a large number of human subjects begin in a discrete region, but may spread to engulf the entire brain, manifest as aperiodic paroxysmal short-lived increases in the power and rhythmicity, in certain frequencies, of neuronal oscillations. Earthquakes are intense bursts of mechanical deformations localized in subarrays of faults embedded within a complex hierarchical network. Although occurring in different media (the earth's crust, not the brain's cortex), earthquakes also manifest as sudden aperiodic oscillations of morphology and spectra similar to seizures, albeit in different frequency ranges reflecting the differences in scale of the excited structures (Fig. 1).

Seizures and earthquakes are the focus of this study for the following reasons: (1) They are definable events, amenable to quantification of their energy and interevent intervals; (2) the systems that generate them have not been experimentally simplified or dimensionally reduced; and (3) good quality and sufficient data are available for the tasks at hand. These considerations circumvent, partially if not wholly, the limitations incurred in the aforereferenced publications.

B. Seizures in humans and earthquake data

Quantitative analyses were performed on:

(1) 81 977 earthquakes between 1984–2000 with magnitude ≥ 2, available in the Southern California Seismic Network (SCSN) catalog. The SCSN gathers its data from a network of over 300 seismic sensors placed throughout Southern California, a subset of shared stations (University of California, Berkeley), and other seismic networks and uses specialized software to detect seismic events. The earthquake catalog information provides a one-line summary of events' parameters and provides fundamental earthquake information including the event's date and time; latitude, longitude, and depth; magnitude; and the event's reference identification number.

(2) 16 032 seizures from continuous multiday voltage recordings directly from the brains of 60 human subjects with mesial temporal and frontal lobe pharmacoresistant epilepsies undergoing surgical evaluation at the University of Kansas Medical Center between 1996 and 2000 with the approval from the Human Subjects Committee and with signed informed consent from each subject. Depth and/or strip or grid electrodes (AdTech, Madison, WI) were either inserted into the brain and/or placed directly over the cortex to record the brain's electrical activity (Electrocorticogram, ECoG); the number of electrodes (48–256) and their placement (unilateral or bilateral temporal and/or frontal) were based on scalp recordings, imaging studies, and neuropsychological testing. Data were collected with commercially available equipment (Nicolet, Madison, WI), filtered (0.5–70 Hz), digitized (10 bits), and stored on a hard drive for off-line processing. All subjects were on reduced dosage of antiseizure medications, a medically accepted practice aimed at increasing the probability of seizure occurrence without altering their site of onset, spectral or clinical characteristics [15,16]. Seizures were localized in space-time and quantified with a validated algorithm [17,18] that estimates the relative increase in median power in the seizure content of the raw signal in the weighted frequency band spanned by a Daubechies mother wavelet (DAUB 4, level 3), which acts as a passband filter (8–42 Hz). This spectral and order sta-

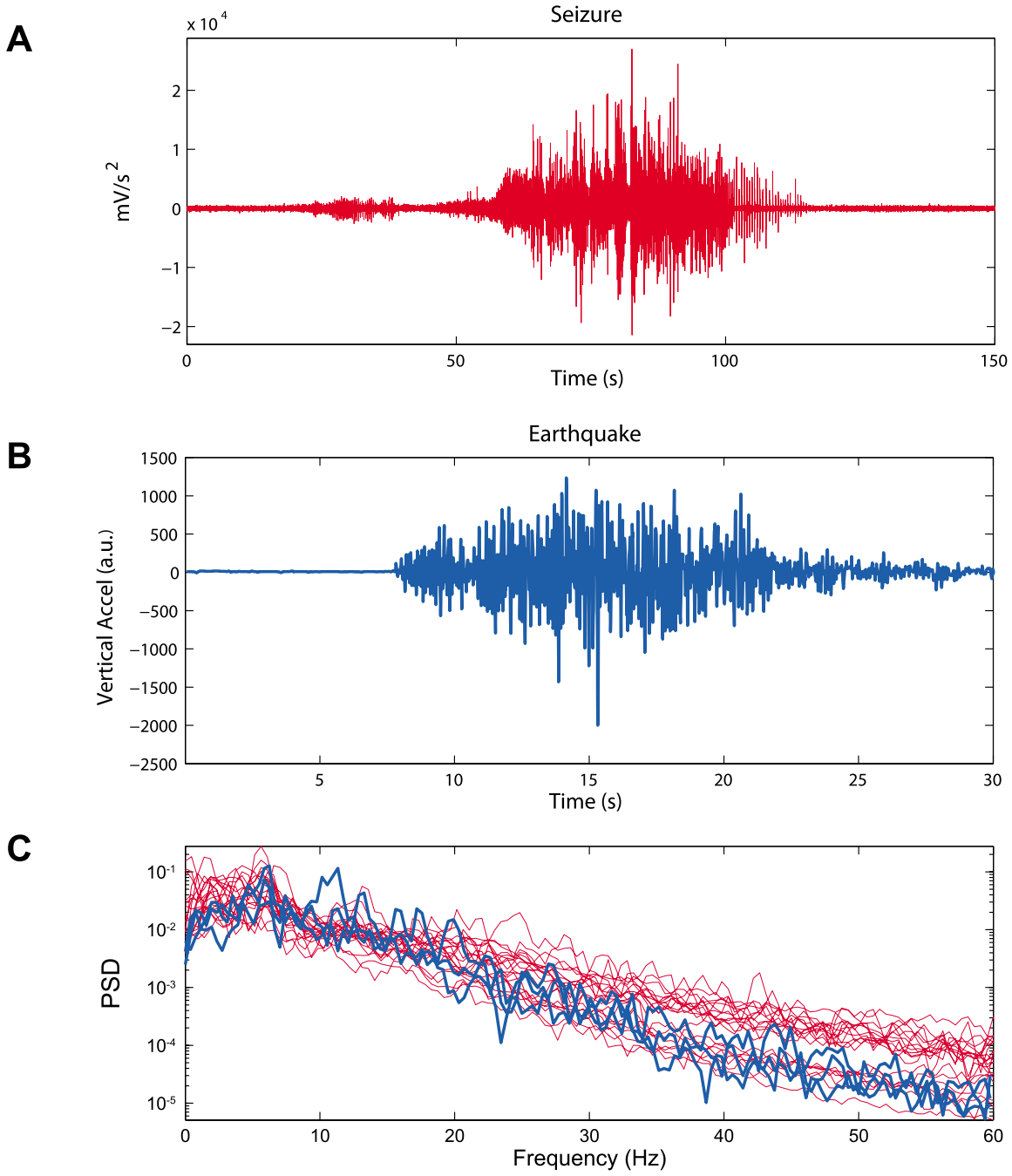

FIG. 1. (Color online) (A) Human electrocorticogram, recorded directly from the brain, containing an intense seizure preceded by a mild one. Data were sampled at 240 Hz; 150 s of data are shown. The second derivative of the signal ("acceleration") is displayed for the both seizures. (B) Vertical acceleration recorded during the October 17, 1989 Loma Prieta earthquake in the Santa Cruz Mountains. Data were sampled at 200 Hz; 30 s of data are shown. (C) Power spectral density estimates for 20 seizures [two each from ten subjects; thin (red) curves] and for the three triaxial acceleration recordings from the Loma Prieta earthquake [thick (blue) curves].

tistics filtering is performed on a foreground window (2 s) whose seizure content is divided by that of an identically filtered background window (30 min). The resulting (dimensionless) ratio R is the updated (present) seizure content (intensity and duration) in the signal. Seizures in this study are operationally defined as paroxysmal increases in relative power (in the 8–42 Hz), reaching or exceeding a ratio (R) value at or above threshold $T=22$ for a duration (in seconds) $D=0.84$ s or more. These constraints ($T=22$, $D=0.84$ s) have been strongly correlated [17,18] with brain activity that epileptologists classify as seizures, either *without* (subclinical) or *with* (clinical) behavioral manifestations. Sites of origin corresponded to those where the electrodes' seizure content *first* reached the $T=22$, $D=0.84$ s values; the spatiotemporal behavior of seizures was tracked using all implanted electrodes.

Seizure durations and intensities obtained with this algorithm were further processed to derive two key features. Sei-

zure "energy" (E) is defined as the product of peak seizure intensity (R_{max}) and duration. This definition is justified because (i) it combines in a single characteristic two complementary natural measures of seizure activity and (ii) it is equivalent to the seismic moment of large earthquakes. Indeed, for earthquakes with rupture lengths larger than the width of the seismogenic crust (about 10 km in Southern California, for instance), the seismic moment scales as the square of the rupture length L [19–21]. Since the duration and the displacement of the earthquake along the rupture are both proportional to L [19], and since the typical amplitude of the radiated seismic waves is proportional to the average displacement [22], the seismic moment is proportional to the product of duration and amplitude of the seismic waves. Our proposed measure of seizure energy is thus directly proportional to the seismic moment ($S \sim 10^{1.5M}$, where M =magnitude). The second feature is the interseizure interval (ISI), defined as the time elapsed between the onset of consecutive seizures, the equivalent of interquake interval. E and ISI values were derived from the site of seizure onset for each subject and only these values were included in the final analyses.

C. Experimental seizure data

Twenty eight adult male (300–450 g) Wistar rats (Charles River Laboratories, Wilmington, MA) were used in this experiment. The animals were kept on 12 h light-dark cycles until the beginning of the experiment and had free access to food and water. These experiments were conducted in compliance with the Guide for the Care and Use of Laboratory Animals, NIH publication 86-23, 1996. On the day of the experiment, rats were preanaesthetized with isoflurane. A subcutaneous injection of 67.5 mg/kg ketamine: 3.4 mg/kg xylazine: 0.67 mg/kg acepromazine was then administered for full anesthesia. Supplemental doses of 100 mg/ml ketamine were given at a rate of 0.2 ml/h to maintain a stable plane of anesthesia. The anaesthetized rat was placed on a stereotaxic instrument (Harvard Apparatus, Holliston, MA, USA) and then connected to a homeothermic blanket control unit (Harvard Apparatus, Holliston, MA) to maintain body temperature at 37.0 ± 0.3 °C. A midline incision was made on the scalp and the skull was exposed. Four sterile electrodes (1 mm outer diameter stainless steel screws) were placed over the cortex for recording of electrical activity. Two of the four electrodes were placed over the right hemisphere 4.2 mm anterior and 5.8 mm posterior and −1.4 mm lateral with respect to bregma; of the remaining electrodes, one was used as a ground and the other as a reference (nasion). Electrode placement was restricted to one hemisphere to minimize trauma and length of surgery; unilateral recordings capture all relevant observables since seizures in this model involve both hemispheres symmetrically and synchronously.

Seizures were induced with 3-mercaptopropionic acid (3-MPA), a compound that blocks the synthesis of gamma-aminobutyric acid (GABA), the main brain inhibitory neurotransmitter. The excitatory-inhibitory imbalance thus created (in the form of a decrease in the GABA/glutamate ratio) results in an increase in interneuronal excitatory coupling, manifesting in generalized seizures. The minimum toxic concentration for 3-MPA (22.2 μg/l) made it difficult to find doses sufficiently high to generate an adequate sample size for statistical analysis without affecting the animal's viability. Two doses and delivery modalities that satisfied these conditions were found and used: nine rats were treated with 70 mg/kg, administered as an intravenous bolus (the "low dose") and 19 received a loading dose of 60 mg/kg followed by a constant intravenous infusion of 50 mg/kg min^{-1} (the "high dose") [23]. Due to the larger power at high frequencies (>30 Hz) in rat seizures compared to those in humans, the detection algorithm parameters were modified [$T=10$, $D=0$ s ($D=0$ means the detection occurs as soon as the seizure energy reached threshold) for rats vs $T=22$, $D=0.84$ s for humans] in an attempt to make the sensitivity and speed of detection equivalent to that in humans.

III. RESULTS

A. "Gutenberg-Richter law"

The pdf's for seizure energy E and for earthquake seismic moment S were estimated using a standard histogram-based method. An adaptive Gaussian kernel-based method [24] gave the same results. The pdf for seizure E follows an approximate power-law distribution, whose slope is equal to the slope of the pdf for S [Gutenberg-Richter law (Fig. 2)] within statistical uncertainties. For both systems, the probability of an event having energy E for seizures (or seismic moment S for earthquakes) larger than x is proportional to $x^{-\beta}$, where $\beta \approx 2/3$ (Fig. 2; see also Table I containing information about the goodness of fit of each curve). For the seismic data, this value of β is found by maximum likelihood estimation [25,26]. For the seizure data, standard linear ordinary least squares (OLS) performed on the logarithm of the binned number as a function of the logarithm of the energy are preferable because the OLS method is less sensitive to the presence of statistical fluctuations and biases at small and large values. The slight deviation from linearity in the pdf of seizure energy (Fig. 2, inset A, red curve and arrow) is due to the presence in this cohort of nine subjects whose energy pdf has characteristic scales (Fig. 2, inset B) resembling those of the upper-left panel of Fig. 7(A) (to be discussed below for its specific meaning), unlike that of the other subjects (51/60) whose pdf follows a power law (Fig. 2, inset A, green curve).

B. Distribution of interevent waiting times

The pdf estimates for interseizure intervals τ were calculated and compared with earthquakes, using a histogram-based estimation method. Both densities approximately follow power-law distributions $\sim 1/\tau^{1+\beta}$ (Fig. 3), with different slopes ($\beta \approx 0.1$ for earthquakes and $\beta \approx 0.5$ for interseizure intervals) (Table I). The difference in slopes should not distract from the more important fact that the pdf's of seizures and earthquake have *fat tails* with exponent $\beta < 1$ indicative of widely broad range of interevent intervals such that both their mean and variance are not well defined. Moreover, recent studies suggest that the pdf of interearthquake intervals

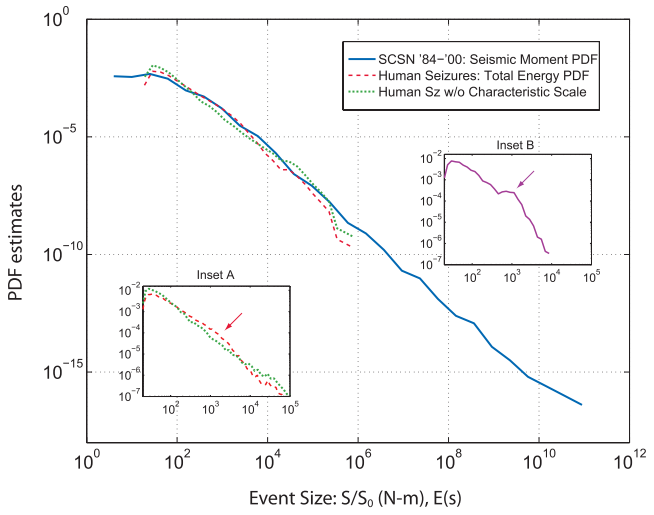

FIG. 2. (Color) Probability density function (pdf) estimates of seismic moments (SCSN catalog; 1984–2000) (blue curve) and of seizure energies of 60 human subjects (red curve) originating from different epileptogenic regions. Both statistics have the same power-law exponent $(1+\beta \approx 1+2/3)$. The red curve has a slight shoulder compared to the green curve. Inset A shows more clearly the shoulder (see arrow) in the pdf estimate of seizure energies (red curve). This shoulder disappears (green curve) with the exclusion of 9/60 subjects whose pdf of seizure energies deviated from linearity. Inset B contains the pdf estimate of seizure energies of one human subject (purple curve) with a prominent shoulder (arrow), suggestive of characteristic scales, which closely resembles that of rats treated with high doses of 3-MPA [Fig. 7(A)]. The pdf of seizures energies of all human subjects (red curve) and of 51/60 (green curve) subjects are shown for comparison (inset A). The seizure scaling range is smaller than for earthquakes, likely due to size differences between the brain and the earth's crust, resulting in drastically different finite-size effects. S, seismic moment; So, seismic moment corresponding to a magnitude zero earthquake; N-m, Newton-meters; E(s), seizure energy.

has several regimes (see Ref. [27] and references therein) and may not be describable by a simple power law. A similar property is likely to apply to the pdf of interseizure intervals.

C. "Omori law" and "inverse Omori law"

Large shallow earthquakes are followed by an increase in seismic activity, which defines their aftershock sequences. Large earthquakes are sometimes preceded by an unusually large activity rate, referred to as a foreshock sequence. The Omori law (Fig. 4) describing the power-law decay $\sim 1/(t-t_c)^p$ (with p close to 1) of the aftershock rate with time elapsed from a mainshock that occurred at t_c was proposed more than one century ago [28] and has since been widely documented [29–32]. Whereas the Omori law describing the aftershock decay rate is one of the few well-established empirical laws in seismology, the increase in the foreshock rate before an earthquake follows the time-symmetric form $-1/(t_c-t)^{p'}$ but only as an average statistical law valid over a large ensemble of events. This is due to the presence of large fluctuations of the foreshock seismicity rate from one mainshock to another and the generally much smaller number of foreshocks compared to the number of aftershocks per mainshock.

When plotting the logarithm of the rate of aftershocks (or foreshocks) as a function of the logarithm $\ln(t-t_c)$ of the time to the mainshock [$\ln(t_c-t)$ for foreshocks], a straight line with slope $-p$ ($-p'$ for foreshocks) should be observed. The aftershock and foreshock exponents p and p' are often claimed to be close to 1, but the universality of their values is still an open question [33–35].

To investigate if seizure behavior resembles the Omori law of earthquake aftershocks, the indicator function of being in seizure was time locked to each end time and averaged at each time point. The resulting curves were normalized by the total fraction of time each subject spent in seizure and then averaged across all subjects. The same steps were followed for the inverse Omori law of foreshocks except that the indicator function was time locked to each seizure onset time. The results (Fig. 4) show an increased probability of other seizures occurring in the window beginning approximately 30 min before a seizure and ending 30 min after a seizure, albeit with steeper slopes than those for earthquakes. A standard foreshock and aftershock selection procedure [36–38] was applied to the earthquake catalog, and a superposed epoch analysis (or stacking) was performed as for the seizure data. Because earthquakes are reported as point events in catalogs, there is no indication to time lock differently for foreshocks and for aftershocks. The stacking of earthquake sequences yields foreshock and aftershock probability increases with qualitatively similar Omori-like time dependencies, but on longer time scales (over about 25 days for foreshocks and more than 30 days for aftershocks). For earthquakes, the observation of aftershocks above a background seismicity rate is known to hold from minutes to more than a century after the mainshock [as exemplified by the notorious 1891 Nobi (Mino-Owari) earthquake in central Japan, whose aftershocks are still detectable at the time of this writing]. The detected duration of aftershock sequences depends on the mainshock magnitude as well as the characteristics of the tectonic environment.

A striking feature in Fig. 4 is the asymmetry of the foreshock and aftershock rates for earthquakes compared with the almost complete symmetry of the "foreshock and aftershock" rates for seizures. In the case of earthquakes, the foreshock and aftershock asymmetry underscores the great difficulty in predicting main shocks, while accurate prediction of aftershocks is now commonplace since they are more numerous, last longer than foreshocks, and their triggering pattern is rather well understood. The difficulty in predicting main shocks is in part attributable to the scarcity of foreshocks and their close temporal proximity to the main shocks. The uncovered symmetry for seizure rates before and after a seizure lends itself to greater predictability vis-à-vis earthquakes.

D. Expected time until the next event, conditioned on the time elapsed since the last one

Davis *et al.* [39] showed the paradoxical result that, for heavy-tailed distributions of interquake intervals such as

TABLE I. Information about probability density function estimates shown in Figs. 2 and 7. Column 3 shows the values of the slopes for each of the *pdf* of (a) seismic moment, (b) seizure energy of humans and rats, and (c) interevent intervals. Columns 4–7 provide the minimum and maximum values for the X and Y *axes* corresponding to the range over which the linear fit took place (producing the aforementioned slopes). Difference between maxima and minima produces the number of decades in each fit for the X and Y axes. The r^2 values are the correlation coefficients of the data that were fit (over the given range), providing a measure of goodness of linear fit. The description column identifies the particular curve to which the row corresponds. EQ=earthquake, SZ=seizure, IQI=interquake interval, and ISzI=interseizure interval.

Curve	Measured system	Slope	$\ln_{10}(X_{\min})$	$\ln_{10}(X_{\max})$	$\ln_{10}(Y_{\min})$	$\ln_{10}(Y_{\max})$	r^2
Figure 2, blue	EQ	-1.7 ± 0.05	2.6	10.2	−3.2	−15.8	0.9995
Figure 2, red	SZ	-1.6 ± 0.05	1.6	5.4	−1.9	−7.9	0.9945
Figure 2, green	SZ	-1.5 ± 0.05	1.5	5.4	−1.9	−7.5	0.9981
Figure 2, inset, red	SZ	-1.6 ± 0.05	1.6	5.4	−1.9	−7.9	0.9945
Figure 2, inset green	SZ	-1.5 ± 0.05	1.5	5.4	−1.9	−7.5	0.9981
Figure 2, inset purple	SZ	-1.6 ± 0.05	1.5	3.9	−1.8	−5.6	0.9639
Figure 3, (thick line)	EQ	-1.0 ± 0.05	2.2	7.8	−3.3	−9.0	0.9991
Figure 3, (thin line)	SZ	-1.4 ± 0.05	1.0	4.9	−1.5	−7.1	0.9977
Figure 7(A)	SZ	-1.0 ± 0.05	−0.9	2.8	1.0	−2.8	0.9952
Figure 7(A), inset	SZ	-1.1 ± 0.05	−0.6	2.8	−0.2	−4.0	0.9994
Figure 7(B)	SZ	-1.2 ± 0.05	−1.7	2.5	2.2	−3.0	0.9637

those shown in Fig. 3, "the longer it has been since the last event, the longer the expected time till the next." Subsequently, Sornette and Knopoff [40] provided among other results a simple quantification in terms of the conditional waiting time denoted $\langle \tau | t \rangle$. In the same way that the moments $\langle x^n \rangle := \int x^n p(x) dx$ of order n provide a characterization of a distribution $p(x)$ that is complementary to the function $p(x)$ itself, by weighting differently the range of x values for

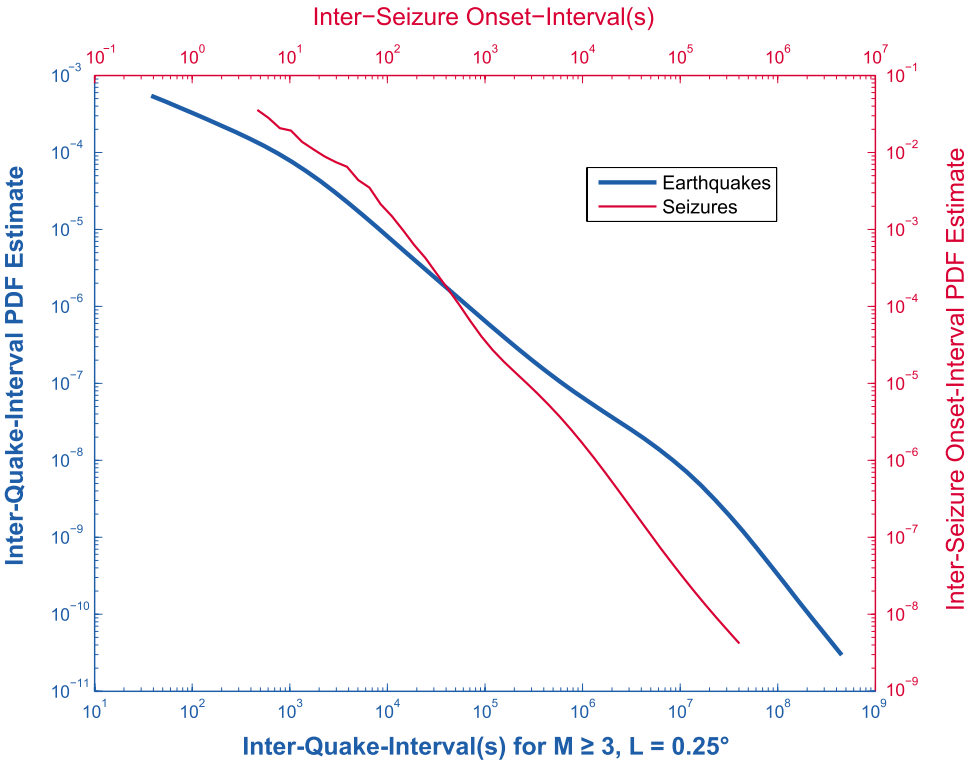

FIG. 3. (Color online) Probability density function estimates of the interevent times between earthquakes (thick curve, lower x axis and left y axis) and seizures in humans (thin curve; upper x axis and right y axis). Earthquakes with return times for events with magnitude ≥ 3 and epicenters within the same cell of a 1° grid in the Southern California Seismic Network catalog were used. For seizures, interdetection interval for all events was used regardless of onset location. M, magnitude; L denotes the longitude and latitude sizes (in degrees) of the smallest "box" used by the SCSN to track earthquakes.

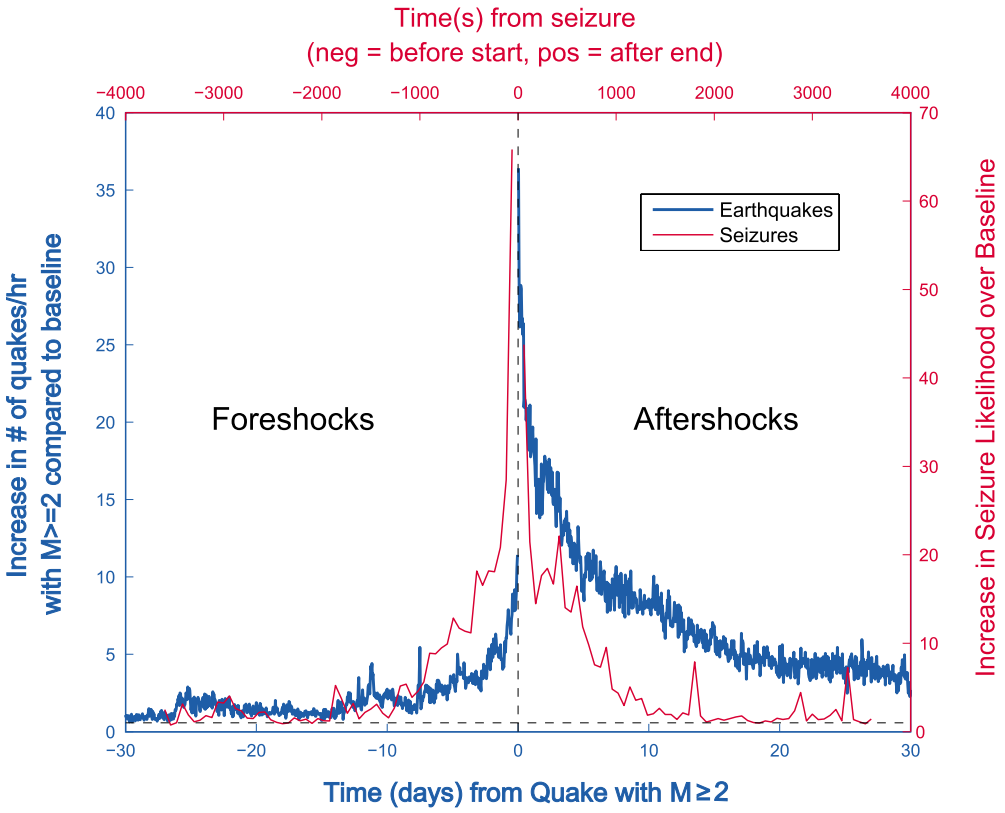

FIG. 4. (Color online) Superimposed epoch analysis of seizures (thin curve; upper x axis and right y axis) and earthquakes (thick curve; lower x axis and left y axis) to test for the existence in seizures of "aftershocks" (Omori-like behavior) and "foreshocks" (inverse Omori-like behavior). Earthquakes with magnitude ≥ 2 preceding and following shock magnitude ≥ 5 are stacked. M, magnitude.

different orders n, the average conditional waiting time $\langle \tau | t \rangle$ until the next event expresses different portions of the distribution of interevent times for different conditioning times t. The statistics $\langle \tau | t \rangle$ complements the characterization of the distribution of interevent waiting times reported in Sec. III B, by providing a nonparametric diagnostic sensitive to deviations from power laws and to crossover regimes [40]. For a power-law distribution, it is easy to show that the dependence of $\langle \tau | t \rangle$ is directly proportional to the time t already elapsed since the last event. This linear dependence of $\langle \tau | t \rangle$ as a function of t is the unique signature of power-law distributions, and it results from their scale invariance property. Furthermore, an increase in $\langle \tau | t \rangle$ as a function of t is an unambiguous nonparametric diagnostic that the tail of the distribution of interevent waiting times is fatter than an exponential. These predictions were tested by computing $\langle \tau | t \rangle$ empirically for each subject's seizures and by comparing it to its analogous statistic in the Southern California earthquake catalog. Figure 5 shows that indeed for both earthquakes and seizures, for short times t since the last event, $\langle \tau | t \rangle$ starts smaller than the (unconditional) average waiting time $\langle \tau \rangle$ between two events and then increases until it becomes significantly larger than $\langle \tau \rangle$ as t increases from the last event. This is a clear nonparametric diagnostic that the distribution of interevent waiting times is indeed "fatter" than exponential and approximately a power law over approximately 2 decades. The saturation and subsequent decay after the peaks is due to finite-size effects for both seizures and earthquakes.

IV. SEIZURE-EARTHQUAKE ANALOGY, COUPLING STRENGTH, AND POWER LAWS IN THRESHOLD OSCILLATOR SYSTEMS

This study uncovers a correspondence, spanning five scale-free statistics between earthquakes and focal seizures in humans that differ (with one exception) only in the precise values of the power-law exponents. This correspondence may be explained on the grounds that both phenomena occur in systems composed of interacting heterogeneous threshold oscillators.

It is perhaps *a priori* counterintuitive to compare earthquakes and seizures (the events), or fault networks and neuron assemblies (the events' supporting elements), due to the systems' large differences in scales and in their constituent matter. Indeed, the textbook model of an earthquake represents a single fault slowly loaded by cm/year tectonic deformations until a threshold is reached at which meter-scale displacements occur in seconds. This ignores the recent realization that earthquakes do not occur in isolation but are part of a complex multiscale organization in which earthquakes occur continuously at all spatiotemporal scales according to a highly intermittent frequent energy release process [34,41]. Indeed, the earth crust is in continuous jerky motion almost everywhere, but due to the relative scarcity of recording devices only the few sufficiently large ones are detected, appearing as isolated events. In this sense, the dynamics of earthquakes is not dissimilar to the persistent barrages of

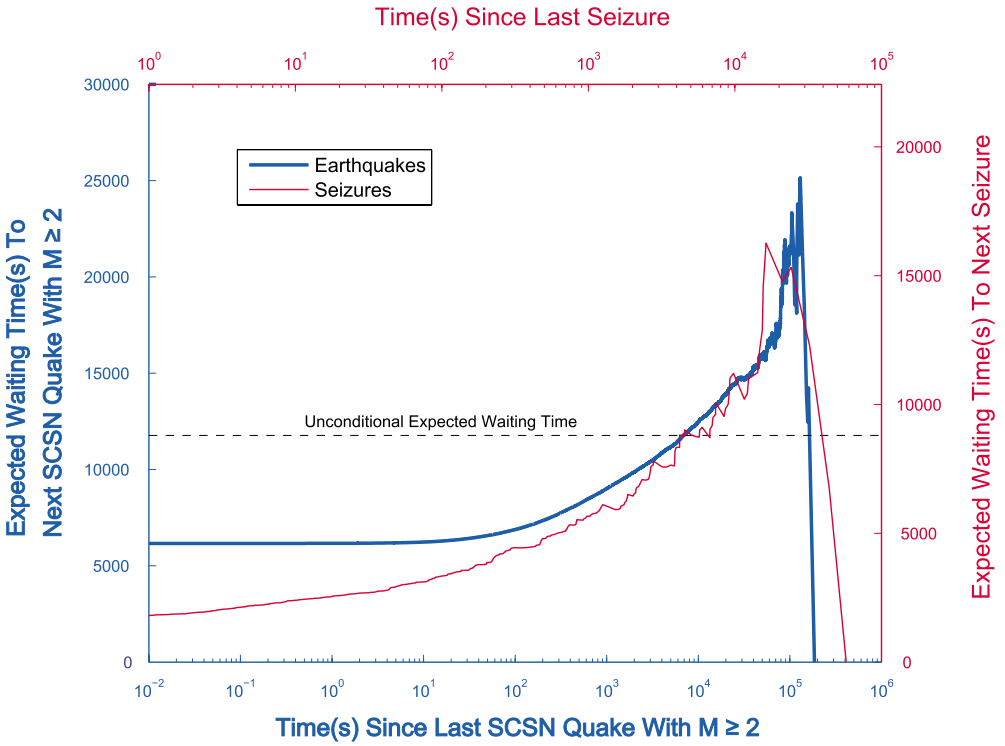

FIG. 5. (Color online) Average conditional waiting time $\langle \tau | t \rangle$ until the next event conditioned on the time t already elapsed since the last event ended. Seizures (thin curve; upper x axis and right y axis); earthquakes (thick curve; lower x axis and left y axis). For seizures and earthquakes, $\langle \tau | t \rangle$ increases paradoxically with t up to a maximum (due to finite-size effects). The dashed horizontal line shows the value of the unconditional average waiting time between two events. The increases in $\langle \tau | t \rangle$ with t confirm the heavy-tailed nature of the distribution of interevent times. M, magnitude.

subthreshold oscillations and of action potentials in neurons, which sometimes coalesce into seizures. The separation of time scales in epileptogenic neuronal assemblies is smaller (milliseconds to months) than in fault networks (fraction of seconds to centuries), but the organization of coupled threshold oscillators is not very sensitive to the magnitude of the separation of time scales, as long as there is one, a property that characterizes relaxational processes. The phase diagram in Fig. 6 relies essentially on the existence of a time scale separation between the loading period and the firing event, a separation which need not be more than one order or so in magnitude.

It is well known in statistical physics and in dynamical systems theory that ensembles of interacting heterogeneous threshold oscillators of relaxation generically exhibit self-organized behavior with non-Gaussian statistics [10,42,43]. The existence of a similar power-law distribution of event sizes for these systems has led to the idea of an underlying universal organization principle captured by the sandpile avalanche paradigm and the concept of self-organized criticality [5]. However, the fact that earthquakes and seizures possess a heavy-tailed distribution of event sizes should not be used *a priori* as sole support for a general correspondence, because such one-point power-law statistics can result from many distinct mechanisms [6]. It is the cumulative evidence presented above and in Figs. 1–5 that provides a strong case for the dynamical analogy between earthquakes and seizures.

A generic qualitative phase diagram (Fig. 6) depicts the main different regimes found in systems made of heterogeneous coupled threshold oscillators, such as sandpile models, Burridge-Knopoff block-spring models [7], and earthquake-fault models [8,44,45]: a power-law regime (probably self-organized critical) (Fig. 6, right lower half) is coextensive with one of synchronization [46] with characteristic size events (Fig. 6, upper left half). This phase diagram embodies the principal qualitative modes that result from the "competition" between strong coupling leading to coherence and weak coupling manifesting as incoherence. Coupling (or interaction strength) is dependent, among others, upon features such as the distance between constituent elements (synaptic gap size in the case of neurons), their type (excitatory or inhibitory) and extent of contact, the existence and size of delays in the transmission of signals, as well as their density and flux rate between constituent elements. Heterogeneity, the other determinant of the system's organization, may be present in the natural frequencies of the oscillators (when taken in isolation), in the distribution of the coupling strengths between pairs of oscillators, in the composition and structure of the substrate (earth or neuropil), and in their topology, among others.

As shown in Fig. 6, for very weak coupling and large heterogeneity, the dynamics are incoherent; increasing the coupling strength (and/or decreasing the heterogeneity) leads to the emergence of intermediate coherence and of a power-law regime (SOC). Further increases in coupling strength (and/or decreases in heterogeneity) force the system toward strong coherence or synchronization and periodic behavior.

The specific boundaries between these different regimes depend on the system under study and on the details of the

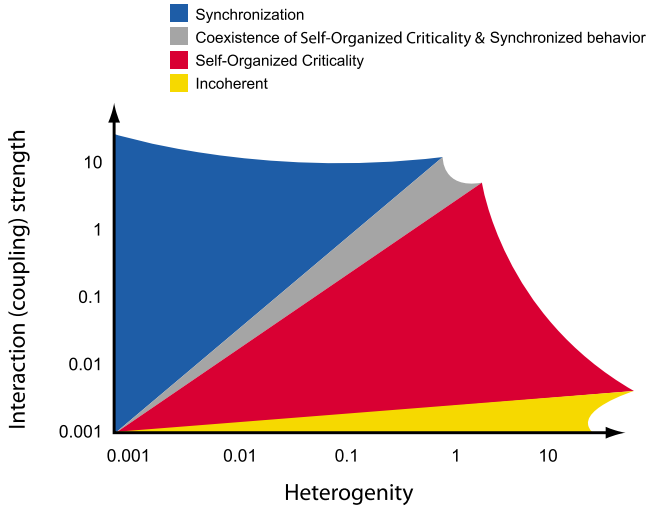

FIG. 6. (Color online) Qualitative phase diagram illustrating the effect of changes in coupling strength (y axis) and heterogeneity (x axis) on the behavior of systems (such as the brain) composed of interacting threshold oscillators (only changes in coupling were investigated in animal models for epileptic seizures). Marked increases in excitatory coupling (*high* 3-MPA dose) drive the system toward the synchronized regime. Slight increases in coupling (*low* 3-MPA dose) drive the system toward the power-law regime indicative of self-organized criticality.

constituting elements and their interactions. In addition, these boundaries may have multiple bifurcations across a hierarchy of partially synchronized regimes within the system. The diagram in Fig. 6 was adapted from the study [8] of a system of coupled fault elements subjected to a slow tectonic loading with quenched disorder in the rupture thresholds. In the SOC regime, the extreme events are not different from smaller ones, making the former unpredictable [47]. In contrast, in the synchronized regime, the extreme events are different, i.e., they are outliers or "dragon kings" [48,49] occurring as a result of some additional amplifying mechanism; these outliers unlike those in the SOC regime are predictable to some degree [50].

V. COUPLING STRENGTH AND THE DYNAMICAL BEHAVIOR OF THE EXCITED BRAIN

The generic phase diagram shown in Fig. 6 leads to the prediction that, if the degree of the *coupling strength* (or of the heterogeneity) between threshold oscillators is manipulated, transitions between the SOC and synchronized regimes will not only occur but will be coextensive. This prediction was tested in rats by increasing the excitatory coupling strength in their brains, since control of neuronal heterogeneity or of coupling strength and heterogeneity in the earth crust is impracticable. Excitatory coupling strength was enhanced with 3-MPA, a compound that blocks GABA synthesis, the main inhibitory neurotransmitter in brain. The seizure energy (E) pdf of nine rats [Fig. 7(A), inset; Table I] treated with low 3-MPA doses (70 mg/kg, bolus injection), so as to only cause a moderate increase in excitatory coupling (relative to untreated rats), a state that corresponds to the weak-coupling power regime (lower half, Fig. 6) of the generic phase diagram, follows a power-law distribution [Fig. 7(A), inset] similar to that shown in Fig. 2, inset A (green curve). In contrast, the energy pdf of 19 rats [Fig. 7(A); Table I] treated with maximally tolerable (for viability) steady-state brain concentrations of 3-MPA (60 mg/kg followed by a constant intravenous infusion of 50 $\mathrm{mg/kg\ min^{-1}}$), a state that corresponds to the strong-coupling regime (Fig. 6, upper half), had power-law (2 decades on the x axis and 3 decades on the y axis; Table I) behavior, coextensive with characteristic scales [Fig. 7(A)]. High 3-MPA concentrations in brain induced very frequent prolonged seizures that violated the linear regime in a log-log scale, forming a "shoulder" [arrow, Fig. 7(A)], indicative of a characteristic seizure size; quasiperiodic behavior is also clearly seen in the seizure foreshock and aftershock plots [Fig. 7(C)] in the shape of regularly spaced (period $\sim$13 s.) oscillations "decorating" the inverse and direct "Omori" laws. The pdf of interseizure intervals also exhibits a clear characteristic time scale (arrow, Fig. 7 lower-left panel) and the average conditional waiting time [Fig. 7(B)] is also highly suggestive of quasiperiodic behavior superimposed on some large waiting time occurrences. These characteristic scales are genuine and unlikely to be recording or analysis artifacts, or unrelated to changes in neuronal dynamics for the following reasons: (i) they were dependent on the dose of 3-MPA whose concentrations in brain were measured using microdialysis [23] and found to be reproducible and highly similar for each of the two dosing schemes and (ii) all reasonable measures were taken to ensure that the experiments, recording, and analyses were performed under the same conditions and 3-MPA concentration was the only parameter changed.

The results of manipulating the strength of excitatory interneuronal coupling with 3-MPA furnish evidence in support of the concepts illustrated in the generic phase diagram (Fig. 6): modest increases in coupling strength manifest as scale-free events, which are likely the expression of SOC, while marked increases generate events with characteristic scales (i.e., periodic) advocating yet another prediction: seizures with characteristic scales should also be observable in humans, as their epileptogenic brain explores the strong excitatory coupling state. The existence of such a regime was uncovered in a human subject (Fig. 2, inset B) buttressing the argument that, as predicted and observed in animals and humans, scale free is not the only behavior of systems populated by relaxation threshold oscillators (neurons in this case). In particular, increases in interneuronal excitatory coupling generate characteristic scale seizures regimes that coexist in space-time with scale-free ones, revealing the richness and complexity of pathological dynamics in the mammalian brain, succinctly captured by the qualitative phase diagram (Fig. 6).

VI. DISCUSSION

The results of this study obtained in intact brains (1) lend credence to the claims [2–9] of dynamical similarities between systems, specifically the epileptic brain and earth crust, that while multifarious in many respects, share one

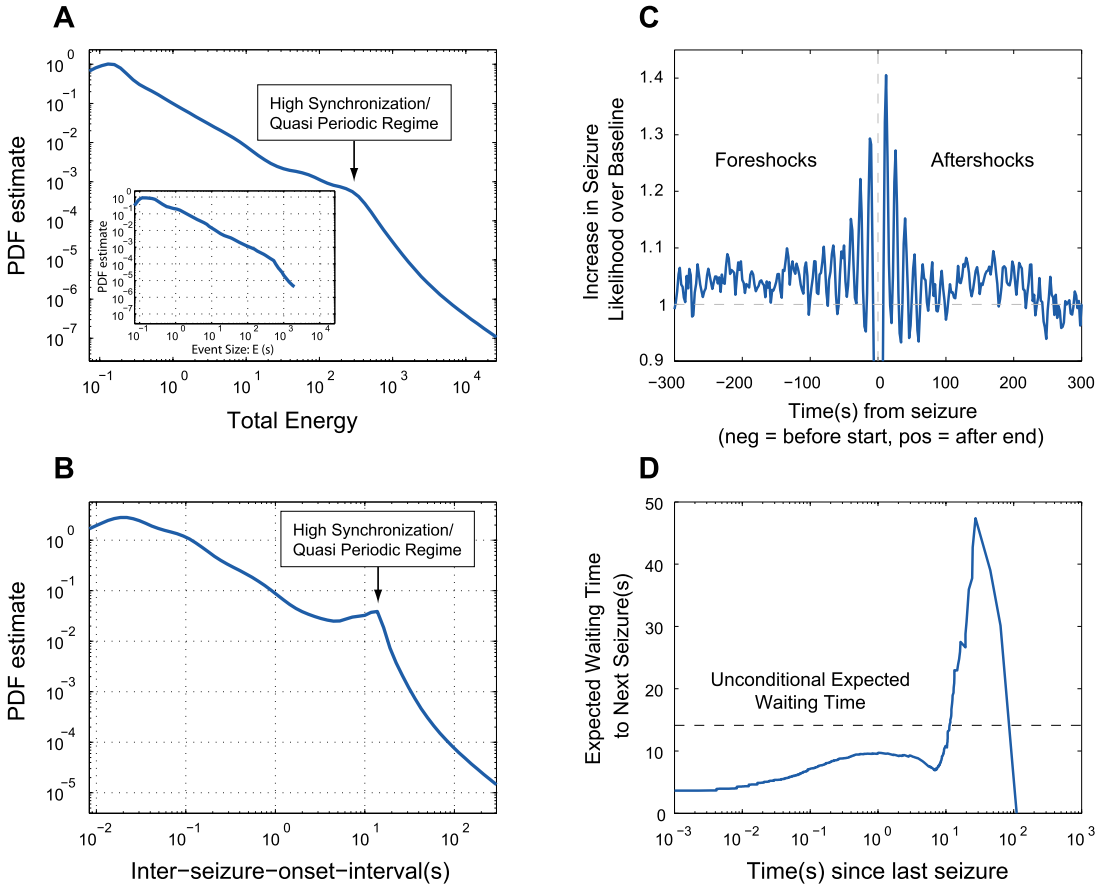

FIG. 7. (Color online) Same statistics as those reported for humans (Figs. 2–4), but for rats treated with a compound (3-MPA) that induces seizures. (A) The pdf estimates of seizure energies recorded from 19 rats treated with high doses (60 mg/kg followed by a constant intravenous infusion of 50 mg/kg min^{-1}), of 3-MPA, show a power law *and* a characteristic size scale regimes. Inset: the pdf estimate of seizure energies of rats treated with low doses (70 mg/kg, single dose) of 3-MPA follows a power law, unlike that of rats treated with high doses (60 mg/kg bolus followed by a constant intravenous infusion of 50 mg/kg min^{-1}) of this compound. (B) Probability density function estimates of interseizure waiting times for the same rats. (C) The "foreshock-aftershock" diagram shows seizure clustering, "decorated" by oscillations (period ~13 s), reflecting strong neuronal coupling. (D) The expected waiting time, conditioned on time since last seizure, is symptomatic of quasiperiodic and self-organized criticality regimes coextensive within the same system.

important commonality: they are composed of interacting (coupled) nonlinear relaxational threshold oscillators and are also "far from equilibrium;" (2) suggest the existence in these systems of a complex rich and "fluid" dynamical "repertoire" in the form of multiple regimes (from highly synchronized to asynchronous through "intermediate" synchrony and SOC) as illustrated simplistically in the phase diagram (Fig. 6); and (3) identify and specify qualitatively and, where possible, quantitatively the commonality features (e.g., pdf of energies and interevent intervals, etc.) between seizures and earthquakes.

One of the central findings of this work related to the peculiarities of dynamical correspondences between seizures and earthquakes in that one statistic (the pdf of seismic moment and seizure energy) share the same exponent, while the other four differ only with respect to their exponents. Differences in constituting elements (organic vs inorganic), in scale, and in other physical properties between the earth and mammalian brain may account for the dissimilarities in the values of the four other statistics (pdf of interevent intervals, Omori and inverse Omori laws, and time until next event). The other central finding is that scale invariance in seizure energy and intervals supports the notion that, at or near a critical point, the epileptic brain's component elements (neurons) are correlated over all existing spatial scales (minicolumns, columns, macrocolumns, etc.) and temporal scales (microseconds, seconds, tens of seconds, etc.). Similarly the pdf of waiting times between successive seizures and between earthquakes have fat tails, indicative of a broad range of interevent intervals such that both their mean and variance are not well defined.

A reasonable interpretation of the Omori and inverse Omori laws and time until next event, as applicable to seizures in humans and in the rat model, and a small body of literature, [14,51] supports the controversial but poorly tested hypothesis put forth one century ago that "seizures beget seizures" [52]. Accurate characterization of the spatiotemporal behavior of seizures is unlikely to materialize if the bases for rejecting this hypothesis continue to be dissociated from the scientific process. Additionally, dynamical as well as practical implications of the impact of the observation, if confirmed, that the pdf of seizure energy and intervals have

fat tails must lead to a reassessment of the statistical methods presently used for the assessment of efficacy of therapies, since they are suitable only for distributions with a well-defined variance such as Gaussian distributions.

The observation of "precursory" seizures (equivalent to earthquake foreshocks) is particularly striking, as it uncovers the potential for real-time forecasts, based on the detection of these "precursors." It is stressed that, for both earthquakes and seizures, the inverse Omori law for foreshocks can only be made apparent by stacking many earthquake or seizure sequences (ensemble analysis), in contrast to aftershock sequences that dominate the seismicity after large earthquakes, emphasizing the statistical rather than deterministic regularity of foreshocks.

Ultraslow (1–100 s) cortical oscillations have been recorded from the intact mammalian brain (e.g., human and rat) [53,54] that could mediate intercortical communication or be the result of subcortical modulation [55]. The presence of ultraslow ($\sim$13 s) regularly recurring cortical oscillations in rats treated with high dose 3-MPA may be a manifestation of widespread cortical synchronization via increased excitatory coupling strength in a maximally driven system; the $\sim$13 s period may be the shortest cycle possible given the neuronal refractory periods, conduction delays, the time required for the synthesis and release of neurotransmitter, and for the generation of high-energy compounds in the presence of markedly elevated metabolic demands.

If confirmed in future studies, the coexistence of distinct epileptic substrates, indicative of SOC and of synchronized regimes (Figs. 2, 6, and 7), not only introduces new challenges, but also provides novel information that may advance seizure prediction. Studies of toy models of coupled heterogeneous threshold oscillators suggest that the level of predictability ought to be different in each of these regimes. A predictor system unable to account for the existence of such possible regime shifts would be obviously ill adapted, would train incorrectly, and would provide incorrect seizure forecasts. The unsuccessful efforts to predict seizures [56–58] may indeed benefit from the "seizure-earthquake analogy" through reference to prediction in seismology which has progressed greatly in recent years. The tangible (but still limited) progress in earthquake prediction is attributable to the development of real-time aftershock hazard models, whose aim is to determine the probability of a large aftershock in the hours following a given mainshock [59]. The collaboratory for the study of earthquake predictability (CSEP) is representative of these new developments, in which open international partnerships support global programs of research on earthquake predictability through prospective comparative testing of scientific prediction hypotheses in a variety of tectonic environments. Prospective 24 h (respectively, 5 years) forecasts of earthquakes of magnitudes larger than 4 (respectively, 5) have been issued in the last few years by 19 different models monitored by the CSEP (see [60] for a recent assessment). Most of these models use in one form or another the emerging understanding of the role of small earthquakes. Until just a few years ago, it was believed that anomalies associated with large earthquakes were the only properties relevant for predictions. While the goal is to predict large events (this is also true for seizures), a growing consensus now recognizes the key role of the myriad of small earthquakes, many of them undetected by standard recording networks, in triggering large earthquakes. Assimilation of this insight into epileptology would dictate that the full hierarchy of events, including what is traditionally classified as single spikes and bursts of spikes, be incorporated along with seizures into prediction models. Promising models used in seismology to account for earthquake occurrences include time-dependent linear as well as nonlinear cascades of clusters (epidemic-type earthquake sequences and its siblings) [33,61,62]. At present, the most popular models are of this type but they are only successful at predicting aftershocks (defined as the events associated with an increase in seismicity following some previous earthquakes), while missing most large events [63]. This discussion would be incomplete without mentioning the long history of searches for signal precursory of an imminent rupture, including foreshocks, strain-rate changes, electric and/or electromagnetic signals, hydrologic changes, geochemical signals, animal behavior, and so on. The few reported successes have been difficult to reproduce perhaps due to the large variety of tectonic settings and the existence of different regimes of seismicity [64]. A promising concept developed early on [65,66] and extended in the last decade views a large earthquake as the culmination of a preparatory phase during which smaller earthquakes smooth out the stress field and express the long-range correlation of stresses that could be associated with the large runaway [67,68]; this corresponds to viewing a large earthquake as a kind of dynamical critical point [69,70], in which accelerated seismic release results from a positive feedback of the seismic activity on its release rate [71]. Future tests of the seizure-earthquake analogy should also involve the question of seismic localization (faults) versus seizure focus/epileptogenic zone as conventionally defined, vs the concept of a distributed epileptic network and its propagation pathways.

In summary, multilayered evidence is provided buttressing the concept that seizures are "quakes of the brain." This justifies an approach to the study of seizure dynamics and forecasting that not only encompasses their intrinsic triggering capacity, but also expands the set of monitored observables from the local (epileptogenic zone or focus) to the global (epileptic network) and from clinical seizures to all types of epileptiform activity (subclinical seizures and other related paroxysmal oscillations), while taking into account the prevailing epileptic state (e.g., SOC vs quasiperiodicity) and the system's history at the time of the forecast. This strategy may bring epileptologists and sufferers closer to one of the "grails" of neuroscience: the prediction and prevention of seizures in humans.

ACKNOWLEDGMENTS

N. Bhavaraju, C. Lunte, and E. Crick provided valuable technical contributions. This work was supported in part by NIH/NINDS Grant No. 5R21NS056022. Y.-C. Lai was supported by ONR, Grant No. N0014-08-1-0627

[1] J. M. Beggs and D. Plenz, J. Neurosci. **23**, 11167 (2003).
[2] N. Goldenfeld, *Lectures on Phase Transitions and the Renormalization Group* (Addison-Wesley, New York, 1993).
[3] M. Ward, *Universality: The Underlying Theory Behind Life, The Universe and Everything* (Pan Books, London, 2002); www.er.ethz.ch/essays/universality
[4] *Extreme Events in Nature and Society: The Frontiers Collection*, edited by S. Albeverio, V. Jentsch, and H. Kantz (Springer, Heidelberg, 2005).
[5] P. Bak, *How Nature Works: The Science of Self-Organized Criticality* (Copernicus, New York, 1996).
[6] D. Sornette, *Critical Phenomena in Natural Sciences*, Springer Series in Synergetics, 2nd ed. (Springer, Heidelberg, 2006).
[7] J. Schmittbuhl, J.-P. Vilotte, and S. Roux, EPL **21**, 375 (1993).
[8] D. Sornette, P. Miltenberger, and C. Vanneste, *Recent Progresses in Statistical Mechanics and Quantum Field Theory* (World Scientific, Singapore, 1995), p. 313.
[9] J. J. Hopfield and A. V. Herz, Proc. Natl. Acad. Sci. U.S.A. **92**, 6655 (1995).
[10] J. B. Rundle, W. Klein, S. Gross, and D. L. Turcotte, Phys. Rev. Lett. **75**, 1658 (1995).
[11] G. A. Worrell, C. A. Stephen, D. Cranstoun, B. Litt, and J. Echauz, NeuroReport **13**, 2017 (2002).
[12] L. M. Parish, G. A. Worrell, S. D. Cranstoun, S. M. Stead, P. Pennell, and B. Litt, Neuroscience **125**, 1069 (2004).
[13] K. Linkenkaer-Hansen, V. V. Nikouline, J. M. Palva, and R. J. Ilmoniemi, J. Neurosci. **21**, 1370 (2001).
[14] I. Osorio, M. G. Frei, D. Sornette, and J. Milton, Eur. J. Neurosci. **30**, 1554 (2009).
[15] S. S. Spencer, D. D. Spencer, P. D. Williamson, and R. H. Mattson, Epilepsia **22**, 297 (1981).
[16] M. G. Marciani and J. Gotman, Epilepsia **27**, 423 (1986).
[17] I. Osorio, M. G. Frei, and S. B. Wilkinson, Epilepsia **39**, 615 (1998).
[18] I. Osorio, M. G. Frei, J. Giftakis, T. Peters, J. Ingram, M. Turnbull, M. Herzog, M. T. Rise, S. Schaffner, R. A. Weinberg, T. S. Walczak, M. W. Risinger, and C. Ajmone-Marsam, Epilepsia **43**, 1522 (2002).
[19] C. H. Scholz, *The Mechanics of Earthquakes and Faulting* (Cambridge University Press, Cambridge, England, 1990).
[20] C. H. Scholz, Bull. Seismol. Soc. Am. **72**, 1 (1994).
[21] D. Sornette and A. Sornette, Bull. Seismol. Soc. Am. **84**, 1679 (1994).
[22] K. Aki and P. Richards, *Quantitative Seismology* (W. H. Freeman, San Francisco, 1980).
[23] E. W. Crick, I. Osorio, N. C. Bhavaraju, T. H. Linz, and C. E. Lunte, Epilepsy Res. **74**, 116 (2007).
[24] K. Cranmer, Comput. Phys. Commun. **136**, 198 (2001).
[25] Y. Y. Kagan, Pure Appl. Geophys. **155**, 537 (1999).
[26] Y. Y. Kagan, Geophys. J. Int. **148**, 520 (2002).
[27] A. Saichev and D. Sornette, J. Geophys. Res. **112**, B04313 (2007).
[28] F. Omori, J. Coll. Sci., Imp. Univ. Tokyo **7**, 111 (1894).
[29] Y. Y. Kagan and L. Knopoff, Geophys. J. R. Astron. Soc. **55**, 67 (1978).
[30] S. D. Davis and C. Frohlich, J. Geophys. Res. **96**, 6335 (1991).
[31] C. Kisslinger and L. M. Jones, J. Geophys. Res. **96**, 11947 (1991).
[32] T. Utsu, Y. Ogata, and R. S. Matsu'ura, J. Phys. Earth **43**, 1 (1995).
[33] A. Helmstetter and D. Sornette, J. Geophys. Res. **108**, 2457 (2003).
[34] G. Ouillon and D. Sornette, J. Geophys. Res. **110**, B04306 (2005).
[35] G. Ouillon, E. Ribeiro, and D. Sornette, Geophys. J. Int. **178**, 215 (2009).
[36] A. Helmstetter, Y. Kagan, and D. Jackson, J. Geophys. Res. **110**, B05S08 (2005).
[37] A. Helmstetter, D. Sornette, and J. R. Grasso, J. Geophys. Res. **108**, 2046 (2003).
[38] A. Corral, Phys. Rev. Lett. **92**, 108501 (2004).
[39] P. M. Davis, D. D. Jackson, and Y. Y. Kagan, Bull. Seismol. Soc. Am. **79**, 1439 (1989).
[40] D. Sornette and L. Knopoff, Bull. Seismol. Soc. Am. **87**, 789 (1997).
[41] Y. Y. Kagan, Physica D **77**, 160 (1994).
[42] X. W. Zhao and T. L. Chen, Phys. Rev. E **65**, 026114 (2002).
[43] P. G. Kapiris, J. Polygiannakis, X. Li, X. Yao, and K. A. Eftaxias, EPL **69**, 657 (2005).
[44] D. Sornette, P. Miltenberger, and C. Vanneste, Pure Appl. Geophys. **142**, 491 (1994).
[45] K. Dahmen, D. Ertas, and Y. Ben-Zion, Phys. Rev. E **58**, 1494 (1998).
[46] S. H. Strogatz, *Sync: How Order Emerges from Chaos in the Universe, Nature, and Daily Life* (Hyperion, New York, 2004).
[47] N. N. Taleb, *The Black Swan: The Impact of the Highly Improbable* (Random House, New York, 2007).
[48] J. Laherrère and D. Sornette, Eur. Phys. J. B **2**, 525 (1998).
[49] D. Sornette, Int. J. Terraspace Sci. Eng. **2**, 1 (2009).
[50] D. Sornette, Proc. Natl. Acad. Sci. U.S.A. **99**, 2522 (2002).
[51] Y. Ben-Ari, Crit. Rev. Neurobiol. **18**, 135 (2006).
[52] W. R. Gowers, *Epilepsy and Other Chronic Convulsive Diseases: Their Causes, Symptoms and Treatment* (Churchill, London, 1901).
[53] N. A. Aladjalova, Nature (London) **179**, 957 (1957).
[54] Y. Nir *et al.*, Nat. Neurosci. **11**, 1100 (2008).
[55] P. J. Drew, J. F. Duyn, E. Golanov, and D. Kleinfeld, Nat. Neurosci. **11**, 991 (2008).
[56] Y. C. Lai, Mary Ann F. Harrison, M. G. Frei, and I. Osorio, Phys. Rev. Lett. **91**, 068102 (2003).
[57] M. A. F. Harrison, I. Osorio, M. Frei, S. Asuri, and Y. C. Lai, Chaos **15**, 033106 (2005).
[58] F. Mormann, R. G. Andrzejak, C. E. Elger, and K. Lehnertz, Brain **130**, 314 (2007).
[59] J. Woessner, S. Hainzl, W. Marzocchi, M. J. Werner, F. Catalli, B. Enescu, A. M. Lombardi, M. Cocco, M. C. Gerstenberger, and S. Wiemer (unpublished).
[60] D. Schorlemmer, J. D. Zechar, M. J. Werner, E. H. Field, D. D. Jackson, and T. H. Jordan, Evison Symposium Special Issue of Pure Appl. Geophys. (to be published).
[61] Y. Ogata, J. Am. Stat. Assoc. **83**, 9 (1988).
[62] A. Helmstetter and D. Sornette, J. Geophys. Res. **107**, 2237 (2002).
[63] D. Sornette and G. Ouillon, Phys. Rev. Lett. **94**, 038501 (2005).
[64] Y. Ben-Zion, M. Eneva, and Y. Liu, J. Geophys. Res. **108**, 2307 (2003).
[65] V. I. Keilis-Borok and L. N. Malinovskaya, J. Geophys. Res. **69**, 3019 (1964).

[66] K. Mogi, *Earthquake Prediction* (Academic Press, Tokyo, 1985).

[67] V. Kossobokov and P. Shebalin, in *Nonlinear Dynamics of the Lithosphere and Earthquake Prediction*, edited by V. I. Keilis-Borok and A. A. Soloviev (Springer, New York, 2002), p. 141.

[68] V. I. Keilis-Borok, P. Shebalin, P. A. Gabrielov, and D. Turcotte, Phys. Earth Planet. Inter. **145**, 75 (2004).

[69] D. D. Bowman, G. Ouillon, C. G. Sammis, A. Sornette, and D. Sornette, J. Geophys. Res. **103**, 24359 (1998).

[70] S. C. Jaumé and L. R. Sykes, Pure Appl. Geophys. **155**, 279 (1999).

[71] S. G. Sammis and D. Sornette, Proc. Natl. Acad. Sci. U.S.A. **99**, 2501 (2002).